



The shapes of the knots corresponding to the special Hopfions

Xuguang Shi^a

College of Science, Beijing Forestry University, Beijing, China

Received: 1 February 2023 / Accepted: 19 July 2023
© The Author(s) 2023

Abstract Torus knots can be constructed using the Faddeev–Skyrme model. These knots are called Hopfions, whose topology is described by the Hopf charge $C = W_1 W_2$. A string is entangled to form the knot, which is characterized by the linking number Lk , which is the sum of the twisting number Tw and writhing number Wr . In this paper, we investigate the relationships between the knot shapes and Hopfions with different values of (W_1, W_2) . We find the knot shapes are not equivalent to the Hopfions shapes even if they have same topological charge. For Hopfions with the value of (W_1, W_2) , the shapes of the knots change with Euler angle θ . The knots have more writhing structure when θ is smaller. If $W_1 < W_2$ the writhing number cannot totally convert to the twisting number. If $W_1 > W_2$ the writhing number can totally convert to the twisting number.

1 Introduction

In high-energy physics, the Faddeev–Skyrme (FS) model is an $O(3)$ - σ model with four derivative terms, named the Skyrme terms. Numerical results show the model has a rich variety of topological solitons, which are called baby skyrmions. The topological charge of the baby skyrmions is characterized by the homotopy group $\pi_2(S^2) \simeq Z$. For the knot-like solitons on the torus, this topological charge is the lump charge W_1 of each baby Skyrme, which means that the baby Skyrme twists W_1 turns along the toroidal cycles on the torus. A baby skyrmion is just a Hopfion in the FS model without the potential terms. Moreover, the potential terms can be introduced into the FS model to construct complex Hopfions on the basis of baby Skyrms. The Hopfions constructed in the FS model [1–4] are all knot-like solitons on a torus. For example, if the potential is a ferromagnetic potential, the Hopfions can be constructed by twisting a closed

baby skyrmion along poloidal circles [5]. In reference [1], the authors provide a deforming ferromagnetic potential, and construct Hopfions by twisting a sine-Gordon kink into the poloidal cycles along the toroidal cycle. For these reasons, all the torus knots are constructed from Hopfions. Hopfions exist in many physical systems, such as particle physics systems [6, 7], Bose-Einstein condensates [8–10], superconductors [11–14], and bio polynomials [15, 16]. Based on these, Hopfions have become the most important topological concept in many physical fields. As topological objects, Hopfions are described by the Hopf charge. The Hopf charge Q is the product of W_1 and W_2 , where W_1 is the number of twists along the toroidal cycles of the torus and W_2 is the number of twists along the poloidal cycles. Therefore, the type of a particular Hopfions can be represented by (W_1, W_2) .

We can twist and writhe a string to form a knot. The topology of these knots is described by the linking number Lk , which is same as the Hopf charge. The linking number Lk is given by the White–Calugareanu formula $Lk = Tw + Wr$, where Tw is the twisting number and Wr is the writhing number [17–19]. However, Tw and Wr are not the topological numbers or integers. Tw can be converted to Wr , and vice versa. However, the sum of Tw and Wr keeps invariance, and is the topological number. Although all knots can be described in terms of the Hopfions [20, 21], the precise connections between the Hopfions and knot remain unclear [1].

To solve the problem, we entangle a string using Euler rotation to form a knot. By considering $SU(2) \simeq S^3$, two-component complex scalar fields are introduced to describe the knot. The unit tangent vectors of the knot are presented on the basis of the complex scalar fields, and are assumed to be the same as the unit vectors given by the Hopf map under a special condition. This is the bridge to investigating the connection between the Hopfions and knots.

^ae-mail: shixg@bjfu.edu.cn (corresponding author)

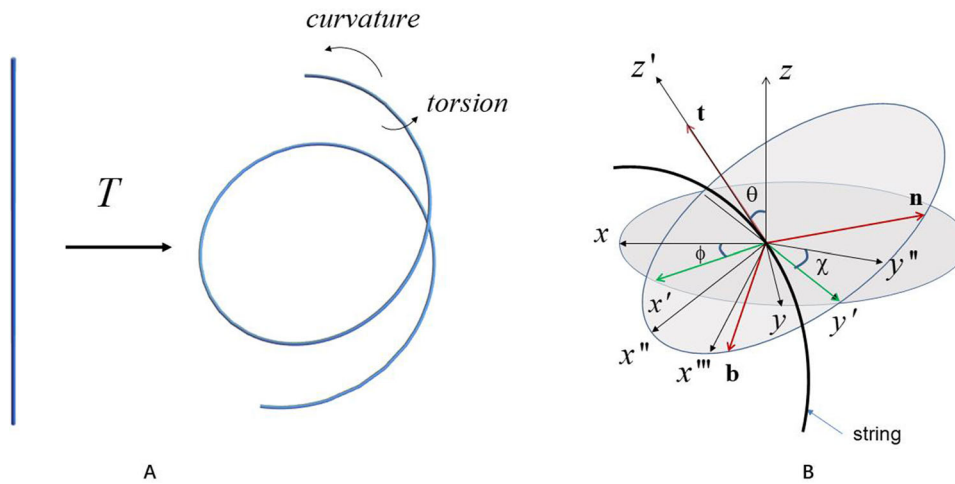


Fig. 1 Euler angles and Euler transformation. **A** Represents a string with torsion and curvature is created when the Euler rotation T operates on a straight line. **B** Shows the Euler angles θ , ϕ , and χ . The first operation is rotating the string about the z -axes by angle ϕ . Thus, we have new

coordinate axes (x', y', z) . The second operation is rotating the string about the new y' -axis by angle θ ; then, we have the axes (x'', y', z') . The last operation is rotating the string about the new z' -axis by angle χ ; thus, we now have the coordinate system (x''', y'', z')

2 The knot and hoptons

We start from a line string. The length l of the string does not affect the topology of the knot. Therefore, we can take the length l as a scalar factor of the string. The knot is represented by $\mathbf{r}(s)$, where s is the arc parameter of the knot. For the line string, we have $\mathbf{r}(s) = (0, 0, 1)$. By considering $SU(2) \simeq S^3$, the knot is described by the two components scalar fields

$$\psi = \begin{pmatrix} 1 \\ 0 \end{pmatrix}. \tag{1}$$

Now we entangle the line string to construct a knot in real space. We introduce the Euler rotation T to represent the twisting and writhing of the string, which is shown in Fig. 1A.

In accordance with $SU(2) \simeq S^3$, the Euler rotation T is written as [22]

$$T = \begin{pmatrix} \cos \frac{\theta}{2} e^{-i \frac{\phi+\chi}{2}} & \sin \frac{\theta}{2} e^{-i \frac{\phi-\chi}{2}} \\ \sin \frac{\theta}{2} e^{i \frac{\phi-\chi}{2}} & \cos \frac{\theta}{2} e^{i \frac{\phi+\chi}{2}} \end{pmatrix}, \tag{2}$$

where θ , ϕ , and χ are the Euler angles, which are functions of the arc parameter s and are shown in Fig. 1B. Letting the Euler rotation T act on the initial two-component scalar field (1), we have the two-component complex scalar field representing the knot:

$$\psi = \left(\cos \frac{\theta}{2} e^{-i \frac{\phi+\chi}{2}} \sin \frac{\theta}{2} e^{i \frac{\phi-\chi}{2}} \right)^t. \tag{3}$$

The knots produced by the Euler transformation are shown in Fig. 2.

The topology of the knots is given by the linking number Lk proposed by Gauss, which is the sum of the indexes of the cross points. From the two-component complex scalar field,

we deduce the unit tangent vectors along the string as

$$\mathbf{n} = \psi^\dagger \boldsymbol{\sigma} \psi = (\sin \theta \cos \phi \sin \theta \sin \phi \cos \theta), \tag{4}$$

where $\boldsymbol{\sigma}$ is the Pauli matrix. In fact, the unit tangent vector maps the curve to a 2-dimensional sphere, that is:

$$\mathbf{n} : \text{curve} \rightarrow S^2. \tag{5}$$

The unit tangent vector satisfies $\mathbf{n} \cdot \mathbf{n} = 1$. To find the meanings of the Euler angles, we consider the deforming $O(3) - \sigma$ model. It is given as:

$$\ell = (\partial_i \mathbf{n})^2 + \frac{1}{36} (\mathbf{n} \cdot \mathbf{J})^2. \tag{6}$$

\mathbf{J} is the spin current [23], which is defined as

$$\mathbf{J} = \nabla \psi^\dagger \boldsymbol{\sigma} \psi - \psi^\dagger \boldsymbol{\sigma} \nabla \psi, \tag{7}$$

where $\boldsymbol{\sigma}$ is the Pauli matrix. Recalling the arc parameter s , (7) is given as

$$\tilde{\mathbf{J}} = \left(\frac{d\psi^\dagger}{ds} \boldsymbol{\sigma} \psi - \psi^\dagger \boldsymbol{\sigma} \frac{d\psi}{ds} \right) \frac{ds}{dx_i}, \tag{8}$$

And (6) is rewritten as

$$\ell = \left[\left(\frac{d\mathbf{n}}{ds} \right)^2 + \frac{1}{36} (\mathbf{n} \cdot \tilde{\mathbf{J}})^2 \right] \left(\frac{ds}{dx_i} \right)^2. \tag{9}$$

Putting (3) and (4) into (9), we find the first term of (9) is

$$\left(\frac{d\mathbf{n}}{ds} \right)^2 = \left(\frac{d\theta}{ds} \right)^2 + \left(\frac{d\phi}{ds} \sin \theta \right)^2. \tag{10}$$

Recalling the theory of surfaces in differential geometry, $\frac{d\theta}{ds}$ is the normal curvature k_n , and $-\frac{d\phi}{ds} \sin \theta$ is the geodesic

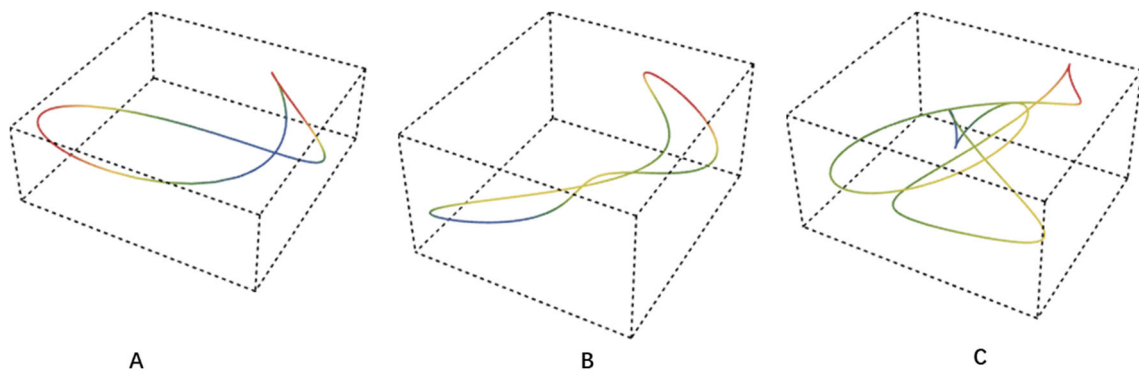


Fig. 2 The knot curves are plotted by referring the equations: $x = \sin(\theta) \cos(\chi) + \cos(\phi) + \sin(\theta) \sin(\chi)$, $y = \sin(\theta) \cos(\phi) + \cos(\chi) + \sin(\theta) \sin(\chi)$, $z = \cos \theta \cos \chi$. Schematic **A** is the knot plot for $\theta = \phi = \chi \in (0, 2\pi)$; **B** is the knot for $\theta \in (0, 4\pi)$, $\phi = \chi \in (0, 2\pi)$; **C** is the knot for $\theta \in (0, 4\pi)$, $\phi \in (0, 6\pi)$, $\chi \in (0, 4\pi)$

curvature k_g [24]. Then, we have

$$\left(\frac{d\mathbf{n}}{ds}\right)^2 = k_n^2 + k_g^2 = k^2, \tag{11}$$

where k is the string curvature. Therefore, the first term represents the bending of the string. The second term of (6) is

$$\frac{1}{36} (\mathbf{n} \cdot \tilde{\mathbf{J}})^2 = \left(\frac{d\phi}{ds} \cos \theta + \frac{d\chi}{ds}\right)^2, \tag{12}$$

where $\frac{d\phi}{ds} \cos \theta$ is the geodesic torsion τ_g of the string. (12) can be rewritten as

$$\frac{1}{36} (\mathbf{n} \cdot \tilde{\mathbf{J}})^2 = \left(\tau_g + \frac{d\chi}{ds}\right)^2. \tag{13}$$

Equations (10)–(13) show the Euler angle θ causes the bending of the string. The Euler angles ϕ and χ produce the torsion of the string. However, θ also contributes to the torsion and ϕ contributes to the string curvature. We calculate the twisting number Tw as

$$Tw = \frac{1}{2\pi} \int_0^L \tau ds = \frac{1}{2\pi} \int_0^L \left(\mathbf{t} \times \frac{d\mathbf{t}}{ds}\right) \cdot \mathbf{n} ds, \tag{14}$$

where τ is the torsion of the string. The unit normal vector \mathbf{t} satisfies

$$\mathbf{t} = \begin{pmatrix} \cos \phi \cos \chi - \cos \theta \sin \phi \sin \chi & -\sin \phi \cos \chi \\ -\cos \theta \cos \phi \sin \chi & \sin \theta \sin \chi \end{pmatrix}. \tag{15}$$

By recalling (12), the torsion τ is

$$\tau = \frac{d\phi}{ds} \cos \theta + \frac{d\chi}{ds}. \tag{16}$$

Then the twisting number is

$$Tw = \frac{1}{2\pi} \int_0^L \left(\frac{d\phi}{ds} \cos \theta + \frac{d\chi}{ds}\right) ds. \tag{17}$$

According to the White–Calugareanu formular $Lk = Tw + Wr$, the writhing number is

$$Wr = Lk - Tw. \tag{18}$$

Moreover, the Eq. (17) shows the angle θ also affects the twisting number. To define the torsion of the space curve, we should provide the unit subnormal vector \mathbf{b} . Then the torsion of the space curve is

$$\tau = \left| \frac{d\mathbf{b}}{ds} \right| \tag{19}$$

The torsion is the rate of change in the unit subnormal vectors with the arc parameter. Therefore, the unit vectors \mathbf{n} , \mathbf{t} , and \mathbf{b} construct the Frenet vector frame. As an example, we plot the cylindrical spiral and build the Frenet vector frame on the spiral in Fig. 3. The 3-dimensional equations of the spiral are given by $x = \sin \theta \cos 3t$, $y = \sin \theta \sin 3t$, and $z = t \cos \theta$. In the first row, $\theta = 0.1\pi$, the angle θ is small, and we find the change in \mathbf{b} (represented by purple arrow) is big. That means the torsion of the cylindrical spiral is high. In the second row, $\theta = 0.4\pi$, the angle θ is bigger. However, the change in \mathbf{b} is smaller. That means the torsion of the cylindrical spiral is smaller. Intuitively, the cylindrical spiral has more writhing structure with large θ than the cylindrical spiral with small θ .

The interesting question is whether knots with different twisting numbers correspond to the same Hopfion types. In order to find the answer, we should construct the Hopfions on the torus domain wall. The Lagrangian density of the FS model is [1,4]

$$\ell = (\partial_i \tilde{\mathbf{n}})^2 + (\partial_i \tilde{\mathbf{n}} \times \partial_j \tilde{\mathbf{n}})^2 + V(\mathbf{n}), \tag{20}$$

where $V(\mathbf{n}) = m^2(1 - n_3)(1 + n_3) - \beta^2 n_1$. The Hopfion is a twisted and closed baby Skyrmion string that is generated by connecting two twisted baby Skyrmion strings. One baby Skyrmion locates at $(0, 0, 1)$ of the sphere, and the other

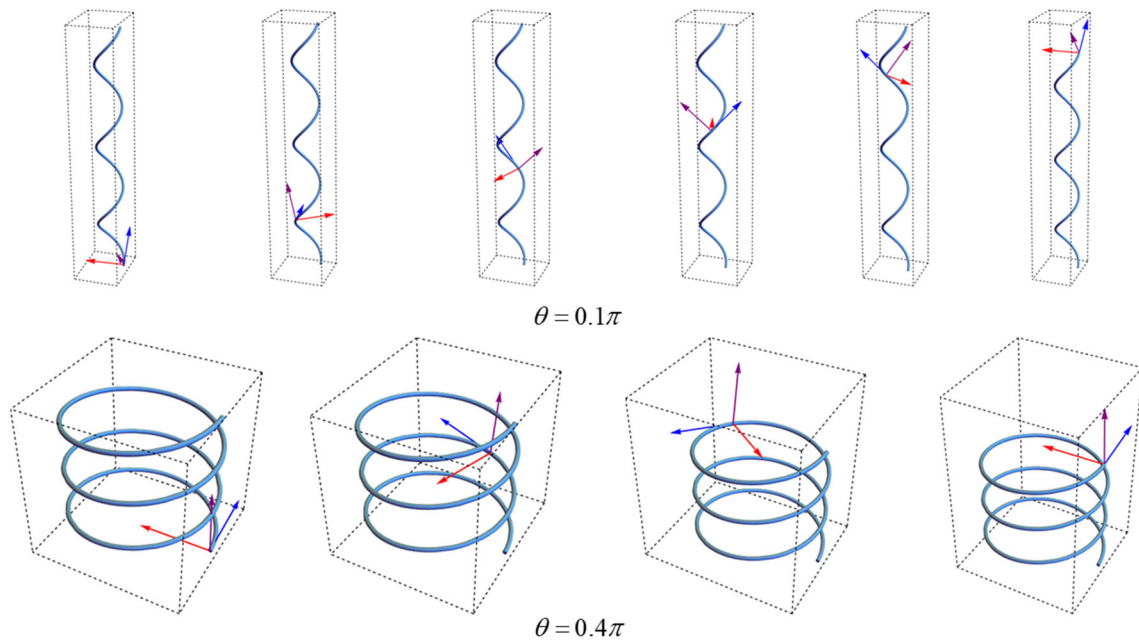


Fig. 3 Conversion between torsion and curvature. We plot a cylindrical spiral and establish the 3-dimensional Frenet unit vectors on it. The first row of the figure is a spiral with $\theta = 0.1\pi$. The second row of the figure is a spiral with $\theta = 0.4\pi$. The Frenet unit vectors \mathbf{n} , \mathbf{t} , and \mathbf{b} are built on the curve. The blue arrow is the unit tangent vector \mathbf{n} ; the

red arrow is the unit normal vector \mathbf{t} ; and the purple arrow is the unit subnormal vector \mathbf{b} . When $\theta = 0.1\pi$, the changes in \mathbf{n} is small, and the changes in \mathbf{b} is big. However, when $\theta = 0.4\pi$, the change in \mathbf{n} is big, and the change in \mathbf{b} is small

locates at $(0, 0, -1)$. In order to describe the Hopfions on the torus domain wall, we introduce the complex scalar field

$$\tilde{\psi} = (\cos \Lambda e^{-iW_1\Phi} \sin \Lambda e^{iW_2\Omega})^t. \tag{21}$$

Based on this ansatz and the Hopf map: $\tilde{\mathbf{n}} = \tilde{\psi}^\dagger \sigma \tilde{\psi}$, the unit vector is deduced as:

$$\tilde{\mathbf{n}} = (\sin 2\Lambda \cos(W_1\Phi + W_2\Omega) \sin 2\Lambda \sin(W_1\Phi + W_2\Omega) \cos 2\Lambda). \tag{22}$$

Hopfions with different Λ values are shown in Fig. 4.

If the map $\tilde{\mathbf{n}}$ is the same as \mathbf{n} , we have the following relations:

$$\begin{aligned} \theta &= 2\Lambda \\ \phi &= W_1\Phi + W_2\Omega. \\ \chi &= W_1\Phi - W_2\Omega \end{aligned} \tag{23}$$

When $\theta = \pi$ and $\Lambda = \frac{\pi}{2}$, the unit vector is $\tilde{\mathbf{n}} = (0, 0, -1)$, which represents the south polar point on the sphere of the Hopf map. When $\theta = 0$ and $\Lambda = 0$, the unit vector is $\tilde{\mathbf{n}} = (0, 0, 1)$, which represents the north polar point. When the equations in (23) are put into (17), and we consider θ is independent of the arc parameter s , the twisting number is

$$\begin{aligned} Tw &= \frac{1}{2\pi} \int_0^{2\pi} W_1 (\cos \theta + 1) d\Phi + \frac{1}{2\pi} \int_0^L W_2 (\cos \theta - 1) d\Omega \\ &= (W_1 + W_2) \cos \theta + (W_1 - W_2) \end{aligned} \tag{24}$$

From this equation, we find the twisting number Tw depends on the numbers W_1 , W_2 and the Euler angle θ .

3 Shapes of knots with given (W_1, W_2)

We consider the Hopf charge $Q = W_1W_2 = 6$. There are four cases: two kinds of trivial knots, one corresponding to $W_1 = 1$ and $W_2 = 6$; and the other to $W_1 = 6$ and $W_2 = 1$. Two kinds of non-trivial knots, one corresponding to $W_1 = 2$ and $W_2 = 3$; and the other to $W_1 = 3$ and $W_2 = 2$. We will plot the shapes of the knots corresponding to the (3, 2) Hopfion after Table 4 because the shapes of these knots are not very complex.

If we consider the trivial knot corresponding to $W_1 = 1$ and $W_2 = 6$, then $W_1 + W_2 = 7$, and $W_1 - W_2 = -5$. The twisting number Tw is

$$Tw = 7 \cos \theta - 5. \tag{25}$$

When $\theta = \pi$, and $\Lambda = \frac{\pi}{2}$, the twisting number is $Tw = -12$. When $\theta = 0$, and $\Lambda = 0$, the twisting number is $Tw = 2$. When $\cos \theta = \frac{5}{7}$, the twisting number is $Tw = 0$. The writhing number Wr is given in Table 1.

If we consider the trivial knot corresponding to $W_1 = 6$ and $W_2 = 1$, then $W_1 + W_2 = 7$, and $W_1 - W_2 = 5$. The

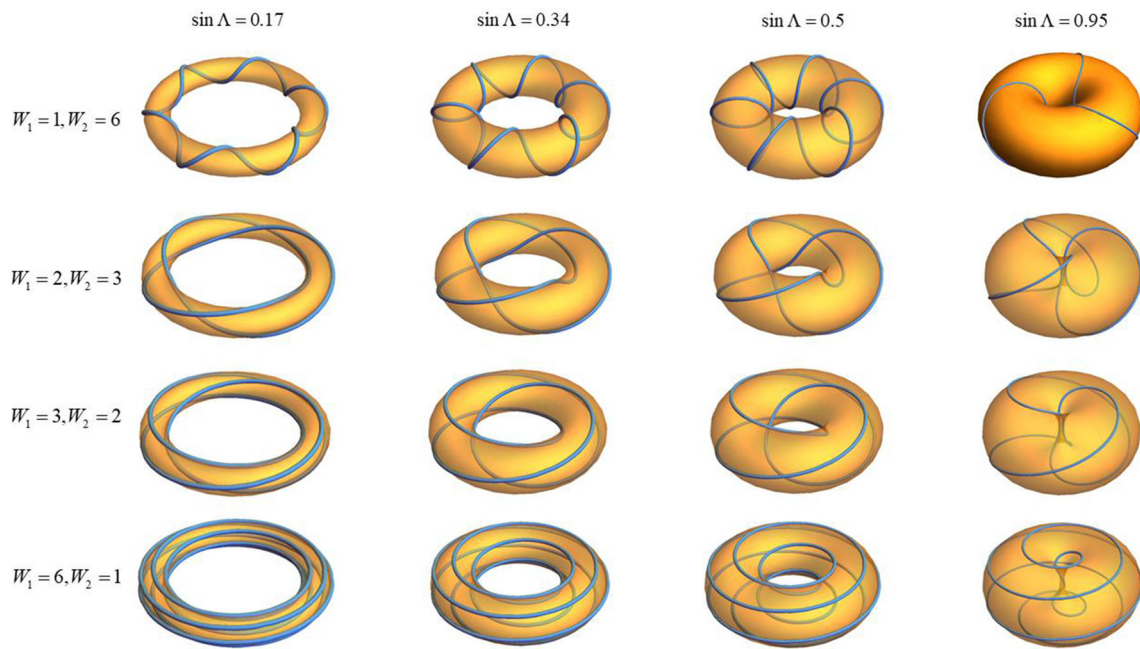


Fig. 4 Hopfions with Hopf charge $C = 6$ are plotted. These are characterized by (W_1, W_2) in the FS model. The Hopfions in the first row of the figure are characterized by $(1, 6)$; the Hopfions in the second row are characterized by $(2, 3)$; the Hopfions in the third row are characterized by $(3, 2)$; and the Hopfions in the fourth row are characterized

by $(6, 1)$. The radius of the torus is definitely related to the Euler angle θ . In this figure, the radius of the torus is $\sin \Lambda = 0.17$ in the first column; $\sin \Lambda = 0.34$ in the second column; $\sin \Lambda = 0.5$ in the third column; $\sin \Lambda = 0.95$ in the fourth column. The type of Hopfions does not change when the radius of the torus changes

Table 1 Hopfions with $W_1 = 1$ and $W_2 = 6$. The conversion between the twisting number and writhing number is presented. The shape of the knot changes with θ . In this condition, the writhing number does not disappear

	$\theta = \pi$	$\theta = \frac{\pi}{2}$	$\theta = \cos^{-1} \frac{5}{7}$	$\theta = 0$
Tw	-12	-5	0	2
Wr	18	11	6	4

Table 2 Hopfions with $W_1 = 6$ and $W_2 = 1$. The shape of the knot changes with θ . In this condition, the writhing number can totally convert to the twisting number

	$\theta = \pi$	$\theta = \cos^{-1}(-\frac{5}{7})$	$\theta = \frac{\pi}{2}$	$\theta = 0$
Tw	-2	0	5	12
Wr	8	6	1	-6

twisting number Tw is

$$Tw = 7 \cos \theta + 5. \tag{26}$$

When $\theta = \pi$, and $\Lambda = \frac{\pi}{2}$, the twisting number is $Tw = 2$. When $\theta = 0$, and $\Lambda = 0$, the twisting number is $Tw = 12$. When $\cos \theta = -\frac{5}{7}$, the twisting number is $Tw = 0$. The writhing number Wr is given in Table 2.

Table 3 Hopfions with $W_1 = 2$ and $W_2 = 3$. The shape of the knot changes with θ . In this condition, the writhing number does not disappear

	$\theta = \pi$	$\theta = \frac{\pi}{2}$	$\theta = \cos^{-1} \frac{1}{5}$	$\theta = 0$
Tw	-6	-1	0	4
Wr	12	7	6	2

Table 4 Hopfions with $W_1 = 3$ and $W_2 = 2$. The shape of the knot changes with θ . In this condition, the writhing number can totally convert to the twisting number

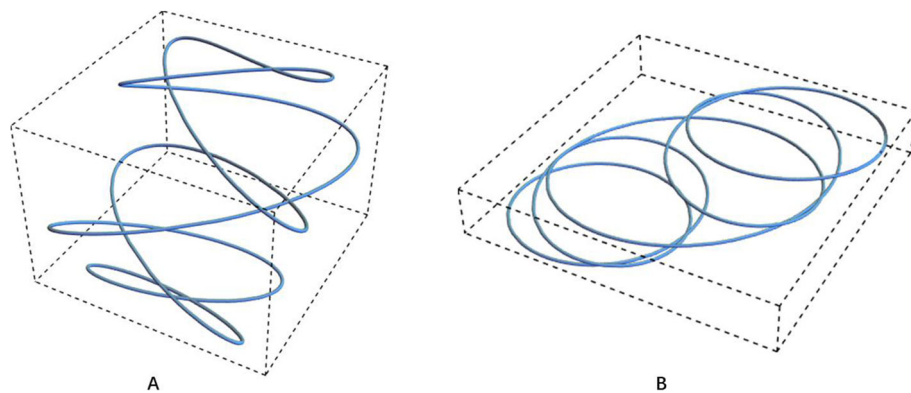
	$\theta = \pi$	$\theta = \cos^{-1}(-\frac{1}{5})$	$\theta = \frac{\pi}{2}$	$\theta = 0$
Tw	-4	0	1	6
Wr	10	6	5	0

Comparing Tables 1 and 2, we find the $(1, 6)$ Hopfion is not equivalent to the $(6, 1)$ Hopfions in view of the conversion between the twisting number and writhing number.

If we consider the non-trivial knot corresponding to $W_1 = 2$ and $W_2 = 3$, then $W_1 + W_2 = 5$, and $W_1 - W_2 = -1$. The twisting number Tw is

$$Tw = 5 \cos \theta - 1. \tag{27}$$

Fig. 5 The shapes of knots with different values of θ are plotted, corresponding to the (3, 2) Hopfion. On the basis of the relation (23), we set $\Phi = \Theta \in (0, 2\pi)$. Then, the equations of the knots are same as the equations given in Fig. 2. **A** Is the knot shape for $\theta = 0$, and we have $Tw = 6$ and $Wr = 0$; **B** Is the knot shape for $\cos \theta = \frac{1}{5}$, and we have $Tw = 0$ and $Wr = 6$



When $\theta = \pi$, and $\Lambda = \frac{\pi}{2}$, the twisting number is $Tw = -6$. When $\theta = 0$, and $\Lambda = 0$, the twisting number is $Tw = 4$. When $\cos \theta = \frac{1}{5}$, the twisting number is $Tw = 0$. The writhing number Wr is given in Table 3.

If we consider the knot corresponding to $W_1 = 3$ and $W_2 = 2$, then $W_1 + W_2 = 5$, and $W_1 - W_2 = 1$. The twisting number Tw is

$$Tw = 5 \cos \theta + 1. \quad (28)$$

When $\theta = \pi$, and $\Lambda = \frac{\pi}{2}$, the twisting number is $Tw = -4$. When $\theta = 0$, and $\Lambda = 0$, the twisting number is $Tw = 6$. When $\cos \theta = -\frac{1}{5}$, the twisting number is $Tw = 0$. The writhing number Wr is given in Table 4.

Similarly, for non-trivial Hopfions, we find a (W_1, W_2) Hopfion is not equivalent to a (W_2, W_1) Hopfion in view of the conversion between the twisting number and writhing number.

Moreover, we find the twisting structure can totally convert to writhing structure if $W_1 > W_2$. The twisting structure cannot totally convert to writhing structure if $W_1 < W_2$. Figure 5 shows the example of knots corresponding to (3, 2) Hopfions with different θ values.

4 Conclusions

In this paper, we found the shapes of knots corresponding to Hopfions characterized by (W_1, W_2) are very complex. There are two reasons: One is the conversion between the twisting number and writhing number, and the other is the Euler angle θ . The Euler angle θ does not decide the type of Hopfion. From Fig. 4, the type of a Hopfion characterized by (W_1, W_2) maintains invariance when θ changes. However, Euler angle θ affects the knot shape, as shown in the tables. Twisting structure converts to writhing structure as θ increases. Moreover, a knot with certain twisting and writhing numbers may correspond to different types of Hopfions. For example, a knot with $Tw = 0$ and $Wr = 6$ may correspond to a (1, 6),

(2, 3), (3, 2), or (6, 1) Hopfion. The Euler angle θ decides which kind of Hopfion is suitable for the knot. We also found the writhing number can convert to the twisting number as θ changes. If $W_1 < W_2$ the writhing number does not disappear as θ changes from 0 to π . The writhing number cannot convert to the twisting number totally. If $W_1 > W_2$ the writhing number can totally convert to the twisting number as θ changes from 0 to π .

Data Availability Statement This manuscript has no associated data or the data will not be deposited. [Authors' comment: All data generated or analysed during this study are included in this published article.]

Declarations

Conflict of interest The authors declare that they have no known competing financial interests or personal relationships that could have appeared to influence the work reported in this paper.

Open Access This article is licensed under a Creative Commons Attribution 4.0 International License, which permits use, sharing, adaptation, distribution and reproduction in any medium or format, as long as you give appropriate credit to the original author(s) and the source, provide a link to the Creative Commons licence, and indicate if changes were made. The images or other third party material in this article are included in the article's Creative Commons licence, unless indicated otherwise in a credit line to the material. If material is not included in the article's Creative Commons licence and your intended use is not permitted by statutory regulation or exceeds the permitted use, you will need to obtain permission directly from the copyright holder. To view a copy of this licence, visit <http://creativecommons.org/licenses/by/4.0/>.

Funded by SCOAP³. SCOAP³ supports the goals of the International Year of Basic Sciences for Sustainable Development.

References

1. M. Kobayashi, M. Nitta, Phys. Lett. B **728**, 314–318 (2014)
2. L. Faddeev, A.J. Niemi, Nature **387**, 58–61 (1997)
3. L.D. Faddeev, Princeton preprint, IAS-75-QS70 (1975)
4. M. Kobayashi, M. Nitta, Nucl. Phys. B **876**, 605–618 (2013)
5. M. Kobayashi, M. Nitta, [arXiv:1304.4737](https://arxiv.org/abs/1304.4737) [hep-th]
6. R.A. Battye, P.M. Sutcliffe, Phys. Rev. Lett. **81**, 4798–4801 (1998)

7. R.A. Battye, P.M. Sutcliffe, Proc. R. Soc. Lond. A **455**, 4305–4331 (1999)
8. Y. Kawaguchi, M. Nitta, M. Ueda, Phys. Rev. Lett. **100**, 180403 (2008)
9. Y. Kawaguchi, M. Nitta, M. Ueda, Phys. Rev. Lett. **101**, 029902 (2008)
10. D.S. Hall, M.W. Ray, K. Tiurev, E. Ruokokoski, A.H. Gheorghe, M. Möttönen, Nat. Phys. **12**, 478–483 (2016)
11. E. Babaev, Phys. Rev. Lett. **88**, 177002 (2002)
12. E. Babaev, Phys. Rev. Lett. **89**, 067001 (2002)
13. E. Babaev, L.D. Faddeev, A. Niemi, Phys. Rev. B **65**, 100512 (2002)
14. F.N. Rybakov, J. Garaud, E. Babaev, Phys. Rev. B **100**, 094515 (2019)
15. Y. Burnier, J. Dorier, A. Stasiak, Nucleic Acids Res. **36**, 4956–4963 (2008)
16. B. Wan, J. Yu, Biophys. J. **121**, 658–669 (2022)
17. J.H. White, Am. J. Math. **91**, 693–728 (1969)
18. F.B. Fuller, Proc. Natl. Acad. Sci. USA **68**, 815–819 (1971)
19. F.B. Fuller, Proc. Natl. Acad. Sci. USA **75**, 3557–3561 (1978)
20. D.W.F. Alves, C. Hoyos, H. Nastase, J. Sonnenschein, Phys. Lett. B **773**, 412–416 (2017)
21. P. Jennings, J. Phys. A **48**, 315401 (2015)
22. J.J. Sakurai, J.J. Napolitano, *Modern Quantum Mechanics* (Addison Wesley, Reading, 2010)
23. Y.-S. Duan, X. Liu, P.-M. Zhang, J. Phys. A **36**, 563–571 (2002)
24. W.H. Chern, *Differential Geometry*, Chinese. (Peking University Publication, Beijing, 1990)